UCRL-11583

UNIVERSITY OF CALIFORNIA
Lawrence Radiation Laboratory
Berkeley, California

AEC Contract No. W-7405-eng-48

Cu

THE MOTION OF DISLOCATIONS IN COPPER SINGLE CRYSTALS

Pierre Petroff
(M. S. Thesis)

September 1964

DISCLAIMER

THIS PAGE

WAS INTENTIONALLY

LEFT BLANK

UCRL-11583

THE MOTION OF DISLOCATIONS IN COPPER SINGLE CRYSTALS

Pierre Petroff

Inorganic Materials Research Division, Lawrence Radiation Laboratory
and Department of Mineral Technology, College of Engineering
University of California, Berkeley, California

Abstract

The motion of two types of dislocation configurations, namely grown in dislocations and punched prismatic loops were studied in copper.

Copper single crystals of 10^5 dislocations per cm^2 were deformed in a cantilever bending test. Grown in dislocations started to move at an average resolved shear stress of 2 g/mm^2. Their multiplication occurred at a stress of 15 g/mm^2 and slip lines appeared at a stress of 38 g/mm^2.

Punched prismatic loops formed by dropping alumina particles on a single crystal have a much smaller mobility. The critical shear stress to move such a loop at room temperature was found to be 200 g/mm^2. The high stress needed to move prismatic loops is probably associated with a high density of jogs on the dislocations.

INTRODUCTION

A knowledge of the behavior of individual dislocations during different stages of deformation of a crystal is important for the development of a physical understanding of the processes of plastic deformation. Chemical etching is one of the most useful experimental means to make possible the direct observation of individual dislocations and their distribution in crystals during various stages of plastic deformation, provided the total dislocation density is less than about 10^7 per cm^2.

Young and Livingstone[1,2] have developed this etching technique for copper crystals; under appropriate etching conditions, the dislocations meeting (110), (100) or (111) surfaces appear as pits of different forms. An etched crystal surface gives therefore a two-dimensional picture of the distribution of dislocations in the crystal. This technique also enables one to follow the motion of dislocations, their multiplication, or the formation of slip lines if the specimen is etched twice, once before and once after deformation. This technique is known as the "double etching technique", and was first used by Gilman on lithium fluoride.[13]

The purpose of the present investigation was to study the motion of two types of dislocations prior to macroscopic yielding: (1) the grown in dislocations existing in an annealed crystal and; (2) prismatic edge dislocation half loops introduced at surfaces by a punching mechanism.

Dislocation motion in copper has been studied previously by Young[1,3] in a three-point bending experiment and by Livingstone[2] in a tension experiment using thick samples. Here the specimens used were very thin .015 in. to .025 in. This was done to make it possible to compare the

behavior of annealed crystals with quenched and aged crystals.

Dislocations produced by a prismatic punching mechanism[4] have been observed in ionic crystals by Barber, Harvey and Mitchell[5]. Loops formed by the same mechanism have also been observed in many metals and alloys; for example, in niobium,[6] magnesium,[7] quenched copper[8] and in Al-Mg alloys.[12]

Dislocation mobility can be estimated from the equilibrium spacing of a set of prismatic loops on the same glide cylinder. Barnes and Mazey in quenched copper,[8] Eikum and Thomas in quench-aged Al-Mg alloys[12] have used Newman and Bullough's theory[9] to calculate the critical shear stress to move a prismatic loop in its glide cylinder.

EXPERIMENTAL PROCEDURE

1. Preparation of the Samples

Copper single crystals of 1 in. diameter and 3 in. length were grown with a random orientation by the Bridgeman method from 99.9999% copper polycrystals.

These crystals, orientated properly on a Laüe camera were cut so that slices having (111) surfaces were obtained by acid sawing. These samples were then chemically polished in a chemical polishing lathe with a solution of (50% HNO_3, 25% H_3PO_4, 25% acetic acid) so that their surfaces were within 2 degrees from the <111> orientation.

By this method rectangular samples of size (0.020 in. x 0.25 in. x 1 in.) were prepared (Fig. 22). Thicker specimens, 0.25 in. x 0.5 in. x 1 in., were used in the punching experiments (see Fig. 22).

All the specimens were annealed at 1075°C for 100 hours. This resulted in a decrease in dislocation density from 10^6 per cm^2 to 10^5 dislocations per cm^2, as determined from etch pit counts.

2. Deformation of the Samples

The crystals were loaded as cantilever beams which had the advantage of causing a gradient of stress along the specimen. Using this method the behavior of dislocations at different stress levels from zero up to the macroscopic yield could be observed.

One end of the crystal was fixed in the grips so that its $[\bar{1}2\bar{1}]$ direction was perpendicular to the bending axis. A known weight was applied by means of a quartz knife on the opposite end. The quartz knife was placed on one arm of an analytical balance (see Fig. 24).

After annealing, and before deformation, the crystals were electropolished at -50°C in a solution:[2,3]

33% HNO_3
67% Methanol .

At 5 volts, 3.4×10^{-6} g/mm^2 of material are removed per minute by electropolishing. Then after a careful rinse in distilled water and in pure alcohol to avoid oxidation, the samples were etched in the solution:[2]

1 part Bromine
15 parts glacial Acetic Acid
25 parts Hydrochloric Acid
90 parts water

for 5 to 7 seconds at room temperature.

After deformation the crystals were re-etched 2 to 3 seconds and rinsed in alcohol. Etch pit observations were made using a Bausch and Lomb metallograph. Dislocations that had moved appear as flat bottom pits of triangular shape. Unmoved dislocations appear as sharp bottomed pits of triangular shape (Fig. 4). Smaller pits, which correspond either to moved dislocations or to new dislocations, can also be distinguished (Fig. 4).

3. Punching of "Rosettes" of Dislocation Loops

Prismatic half loops were produced by dropping alumina balls of 30μ to 40μ diameter on the surface of the sample from a height of 8 inches. On impact they caused a deformation of the crystal similar to that due to differential volume changes around a precipitate during cooling. Thus rows of prismatic dislocation half loops forming "rosettes" were formed.

Prior to impacting the samples were electropolished, rinsed and etched in the etching solution for seven seconds. After impacting the crystals were then re-etched for 3 to 4 seconds and rinsed so that the "rosettes" of loops appeared as new pits when observed. Figures 9 to 21 show the type of deformation surrounding the points of impact. The half loops are probably semi-circular in shape as illustrated schematically in Fig. 26.

Subsequent bending deformation or thermal stresses due to cooling or heating did not appear to change the configuration of half loops in the rosettes.

RESULTS AND DISCUSSION

1. Motion of the Dislocations in an Annealed Sample

The dislocation density in the sample after annealing was 10^5 per cm^2. The percentage N of moved dislocations was studied at different stress levels in each sample by counting the number of flat bottomed pits, N_1 per cm^2, and the number of large sharp pits, N_2 per cm^2 (Figs. 1-6). $N = N_1/N_1 + N_2$ is plotted as a function of the maximum tensile stress for two samples cut from the same crystal in Fig. 29.

The stress was evaluated by the cantilever formula: the tensile stress on the surface of the sample at a distance L from the point of the applied force in the elastically deformed region is

$$\sigma_{max} = \frac{2PL}{a^2 b} ,$$

where a = depth of the sample in mm
b = width of the sample in mm
P = applied load in grams
and σ_{max} = tensile stress in g per mm^2

(see Fig. 25).

The resolved shear stresses σ_R in the principal slip systems for this orientation of the sample (see Fig. 22) are given as a function of σ_{max} in Table I.

Table I. Resolved shear stresses for crystals with $[\bar{1}2\bar{1}]$ tensile axis.

Slip Plane	Slip Direction	σ_R = Resolved Shear Stress
$(\bar{1}11)$	$[0\bar{1}1]$	0.408 σ_{max}
$(11\bar{1})$	$[1\bar{1}0]$	0.408 σ_{max}
$(1\bar{1}1)$	[011] or [110]	0.272 σ_{max}
$(11\bar{1})$	$[\bar{1}0\bar{1}]$	0.272 σ_{max}
$(\bar{1}11)$	$[\bar{1}0\bar{1}]$	0.272 σ_{max}
$(\bar{1}11)$	[110]	0.128 σ_{max}
$(11\bar{1})$	[011]	0.128 σ_{max}

The dislocations will start to move first in the slip systems with the highest resolved shear stress.

Extrapolation to N = 0 (Fig. 29), which corresponds to motion of the first dislocations gives a critical applied tensile stress of 4 g/mm^2 < σ_{max} < 6 g/mm^2. The corresponding resolved shear stress on the most favorably oriented system is σ_R= 2 g/mm^2.

Multiplication of dislocations occurs in two stages. In the first stage, pairs of pits appear along traces of {111} planes; these double pits probably correspond to the bowing out of dislocations to the surface (see Fig. 8). In the second stage sources produce rows of new dislocation pits which also lie along the traces of the slip plane (see Figs. 6-8).

Finally, a broadening of these small slip lines occurs. Multiplication of dislocations was observed at an average resolved shear stress of $\sigma_R = 15\ g/mm^2$.

The results agree fairly well with those obtained by Young.[3] However, he found that 50% of the dislocations moved at a stress of 25 g/mm^2: this experiment indicates that 50% of the dislocations moved at a stress of 20 g/mm^2. In his experiments, Young observed the motion of the grown in dislocations in crystals of 99.999% at an average resolved shear stress of 4 g/mm^2. By using the same definition for multiplication of dislocations as the one used in this experiment, he found a resolved shear stress for multiplication of dislocations of $\sigma = 18\ g/mm^2$. The present results also agree well with the the results of Tinder and Washburn[11] who detected motion of dislocations by sensitive stress-strain measurements at a resolved shear stress of 2 g/mm^2.

2. Motion of Prismatic Loops

For the last loop in a row of prismatic loops on the same glide cylinder the force due to the shear stress $\Sigma\ \tau_i$ associated with the other last loops on the glide cylinder and the force opposing the glide of the last loop must be equal. Therefore, the sum $\Sigma\ \tau_i$ represents the critical shear stress for motion of the dislocation loop. To a close approximation $\Sigma\ \tau_i$ is given by:

$$\tau^* = \sum_{i=1}^{4} \tau_i$$

τ_i = shear stress produced by the i^{th} loop of a row of more than 4 loops. The effect of the loops 5....10 of the row being negligible.

Here we are dealing with half-loops at an external surface. We will assume that the shear stress on the glide cylinder due to a half loop is the same as for a complete prismatic loop. To justify this assumption an interstitial loop in a regular atomic array (Fig. 27) is considered. To a first approximation, for a prismatic loop several microns in diameter, shear stresses are zero at all points of the plane AA' (Fig. 27). Although the normal stress is not zero, it is less than $\frac{G}{10^5}$ at all points. Therefore, if the crystal is cut into 2 parts along this plane no major change in the stress field occurs.

The rows of prismatic half loops produced by impact of alumina spheres always extend along <110> directions. If they are semi-circular in shape, as seems highly probable, then they contain a distribution of jogs as shown in Fig. 26.

Newmann and Bullough[9] considered the interaction of a number of prismatic loops on the same glide cylinder. The shear stress on the glide cylinder, τ, due to a single loop has been evaluated. Their results were given in terms of a dimensionless parameter V which was a function of the loop radius a:

$$\tau = \frac{VbG}{4\pi(1-\nu)}$$

where b = Burgers vector of the loop,
G = Shear modulus,
ν = Poisson's ratio,
and V = Dimensionless parameter obtained from the curve (Fig. 28) given in Bullough's paper.

The shear stress on the glide cylinder due to a single loop as shown in Fig. 28 (reproduced from their paper) decreases rapdily with distance z from the loop. When the ratio $\frac{z}{2a}$ is > 2.5 the critical shear stress is:

$$\tau = \frac{3ba^3G}{(1-\nu)z^4} \quad .$$

To calculate the critical shear stress τ^* necessary to move the last loop of a row of five loops or more we consider the shear stress τ_i created by the i^{th} loop at a distance z_i from the last loop. The critical shear stress to move the last loop will be:

$$\tau^* = \sum_{i=1}^{4} \tau_i(a_i z_i) \quad .$$

For the calculations we have considered only the rows of more than five loops, these loops being well aligned and regularly spaced in each of the considered rows. It was thought that these were cases where there had not been strong interaction with parts of the grown-in dislocation network.

Figures 9, 10 and 11 show typical examples of the kinds of rows used for the calculations. A sample calculation of the critical shear stress is given in the Appendix.

The critical shear stress τ^* to move the last loop was found to vary from 20 g/mm^2 < τ^* < 436 g/mm^2 with an average value of 200 g/mm^2. This large scatter in the values of τ^* may come from the dislocation configuration or surface contour existing in the crystal at the place of impact of the ball. This could affect the shape of the resulting prismatic loops and therefore their jog density. Neither angle of impact of the balls nor application of a static stress during impact was found to affect the distribution or spacing of loops. The size of the "rosettes" at stresses varying from 5 g/mm^2 to 120 g/mm^2 was the same as for unstresses samples (see Figs. 12-17).

Even in the highly deformed regions $90 < \sigma < 120$ g/mm^2 the loops did not move whereas all the other dislocations in the neighborhood had moved and multiplied to form slip lines (see Figs. 16 and 17).

No initiation of slip lines or slip bands was observed near the loops (Fig. 17). The relatively small mobility of these loops is probably due to their shape. Further experiments are needed to determine whether they have a circular shape as observed for smaller prismatic loops or a diamond shape as observed for larger loops.[13]

CONCLUSION

At room temperature the grown in dislocations in an annealed 99.999% copper single crystal with an initial dislocation density of 10^5 per cm^2 start to move at a critical shear stress of about 2 g/mm^2. Dislocation multiplication occurs at a stress of 15 g/mm^2 and the formation of slip lines is observed at a stress of 18 g/mm^2.

At a stress of 20 g/mm^2, 50% of the dislocations have moved. At room temperature, prismatic dislocation loops of a punched type move under an average critical shear stress $\tau^* \approx 200$ g/mm^2. The smaller mobility of these loops compared to the grown in dislocations suggest that they have a heavily jogged circular shape.

Acknowledgements

The author expresses his gratitude to Professor Jack Washburn for his encouragement and continued interest. This research was supported by the U.S. Atomic Energy Commission thrcugh the Inorganic Materials Research Division of the Lawrence Radiation Laboratory.

APPENDIX

Example of Calculation of the Critical Shear Stress to Move a Loop:

The last loop of the upper row of Fig. 18 is considered. Figure 23 gives the dimension of the loops,

$$r = 1.5\ \mu$$
$$d = 4\ \mu\ ,$$

and their spacing. Let us calculate $\tau_1(a_1z_1)$ shear stress applied by loop No. 1 on the last loop of the row:

$$\tau_1(a_1z_1) = \frac{3ba_1^3G}{(1-\nu)z_1^4}$$

$$\tau_1(a_1z_1) = 1.09\times10^{-7}\ G$$

$z_1 = 12\mu$

$a_1 = 1.25\mu$

$b = 2.5\times10^{-4}\ \mu$

$\nu = 0.35$

$\rho_1 > 2.5$

to $\tau_2(a_2z_2)$ shear stress applied by loop No. 2 on the last loop of the row:

$$\tau_2 = \frac{3ba_2^3G}{(1-\nu)z_2^4}$$

$$\tau_2 = 9.5\times10^{-7}\ G$$

$z_2 = 8\mu$

$a_2 = 1.5\mu$

$\rho_2 = 2.566\mu$

to $\tau_3(a_3z_3)$ shear stress applied by loop No. 3 on the last loop of the row:

$$\tau_3(a_3z_3) = \frac{VbG}{4\ a(1-\nu)}$$

$$\tau_3(a_3z_3) = 7.35\times10^{-6}\ G$$

$z_3 = 4\mu$, $\rho_3 = 1.33$

$a_3 = 1.5\mu$, $V = 0.36$

The critical shear stress required to move the last loop is:

$$\tau^* = \tau_1(a_1 z_1) + \tau_2(a_2 z_2) + \tau_3(a_3 z_3) = 8.4 \times 10^{-6}\, G \,.$$

For a value of $G = 8 \times 10^6$ g/mm^2, $\tau^* = 67.28$ g/mm^2.

REFERENCES

1. F. W. Young, J. Appl. Phys., 32, 1815 (1961).
2. J. D. Livingstone, Acta Met., 10, 229 (1962).
3. F. W. Young, J. Appl. Phys., 33, 3553 (1962).
4. F. Seitz, Rev. Mod. Phys., 79, 723 (1953).
5. D. J. Barber, K. B. Harvey and J. W. Mitchell, Phil. Mag., 2, 704 (1957).
6. A. Berghezan and A. Fourdeux, Acad. des Sciences, 462 (1961).
7. P. G. Partridge and S. Lally, to be published.
8. R. S. Barnes and D. J. Mazey, Acta Met., 11, 281 (1963).
9. R. C. Newman and A. Bullough, Phi. Mag., 921 (1960).
10. C. S. Barrett, Structure of Metals, McGraw Hill N., p. 297 (1952).
11. R. Tinder and J. Washburn, Acta Met., 12, 129 (1964).
12. A. Eikum and G. Thomas, Acta Met., 12, 537 (1964).
13. J. J. Gillman and W. G. Johnston, Solid State Physics, 13, 167 (1961).

Figure Captions

Figures 1 through 8 inclusively show dislocation motion and dislocation multiplication at different stress levels.

Fig. 1. Sample A, x500. Dislocation motion at low stresses $\sigma \simeq 8.5$ g/mm^2.

Fig. 2. Sample A, x500. Dislocation motion at stress $\sigma = 14$ g/mm^2.

Fig. 3. Sample A, x500. Dislocation motion at stress $\sigma = 17.5$ g/mm^2.

Fig. 4. Sample A, x500. Dislocation motion at stress $\sigma = 27$ g/mm^2. 44% of the dislocations have moved.

Fig. 5. Sample A, x500. Dislocation motion at stress $\sigma = 34$ g/mm^2. 54% of the dislocations have moved.

Fig. 6. Sample B, x500. Dislocation motion at stress $\sigma > 39$ g/mm^2. The slip lines formation is observed.

Fig. 7. Sample B, x500. Dislocation motion at stress $\sigma = 39$ g/mm^2. Source producing a row of dislocations and initiating a slip line.

Fig. 8. Sample B, x500. Dislocation motion at stress $\sigma = 39$ g/mm^2. Source producing a row of dislocations. Double small pits corresponding to the bowing out of a dislocation.

Figs. 9, 10, 11. Rosettes of punched prismatic loops on an horizontal sample.

Figs. 12, 13, 14. x500, Rosettes of punched loops on a sample at 45°. The length of the row is greater in the direction of maximum impact force.

Fig. 15. x1000. Sample bend with the <110> axis bending the stress applied is $\sigma \simeq 15$ g/mm^2.

Fig. 16. x500. Sample bend with the <110> axis. The stress applied is $\sigma \simeq 30$ g/mm^2.

Fig. 17. x500. Sample bend with a <110> axis. The stress applied is $\sigma = 30$ g/mm^2.

Fig. 18, 19, 20, 21. Sample under thermal stresses: the rosettes were formed at room temperature and etched. The final position of the loops after cooling the sample at -196°C and reheating it at room temperature is indicated by the small pits.

Fig. 22. Shape and orientation of the specimen.

Fig. 23. Dimension of loops in a row of the rosette of the picture, Fig. 18.

Fig. 24. Testing apparatus.

Fig. 25. Distribution of the stresses in a cantilever beam.

Fig. 26. Shape of a semicircular loop lying in a (111) plane.

Fig. 27. Loop of interstitial atoms in a regular atomic array.

Fig. 28. The shear stress distribution on the cylindrical glide surface r = a due to a single loop of radius a and strength b situated at 2 = 0. After Bullough.[9]

Fig. 29. N = % of moved dislocations as a function of the applied tensile stress.

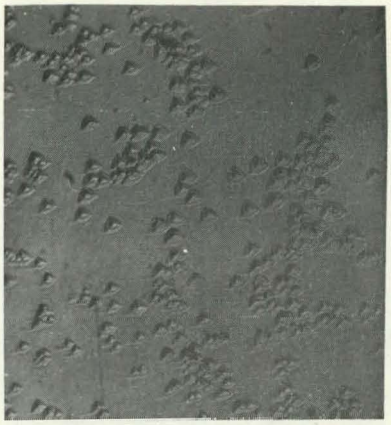

Fig. 1

Fig. 2

Fig. 3

Fig. 4

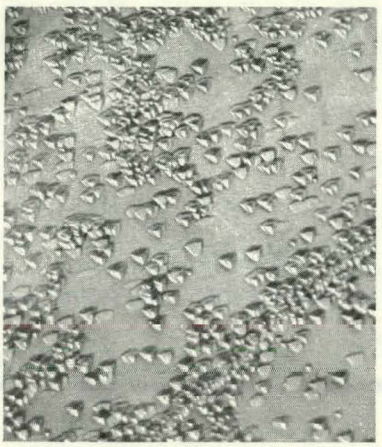

Fig. 5

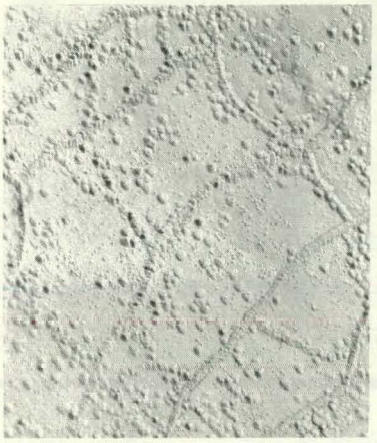

Fig 6

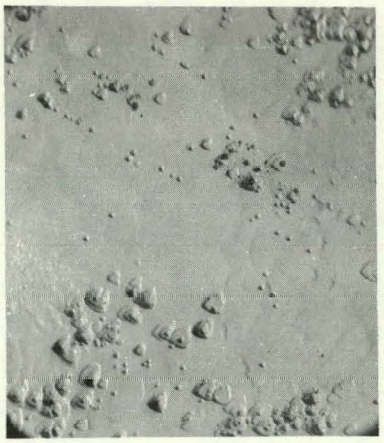

Fig. 7

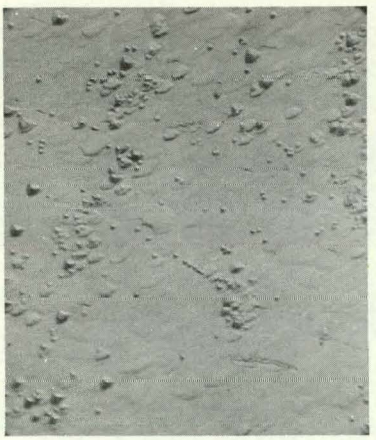

Fig. 8

ZN-4502

Fig. 9

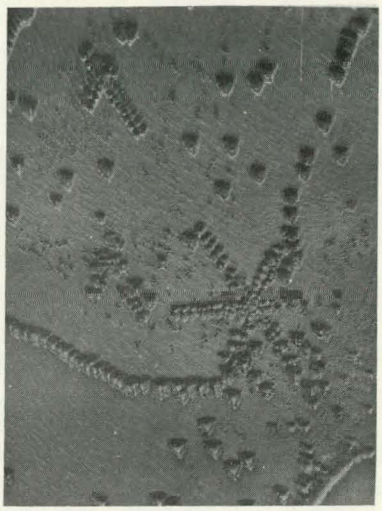

Fig. 10

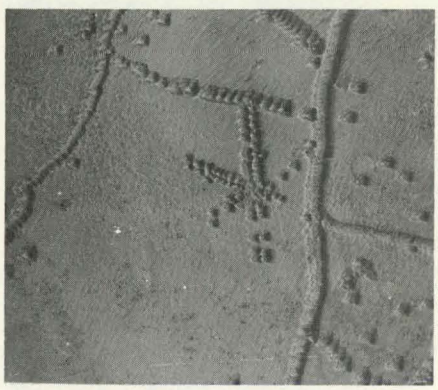

Fig. 11

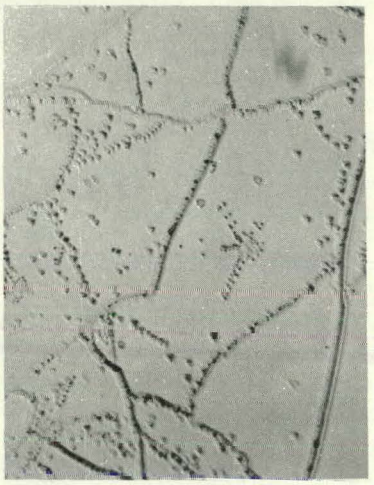

Fig. 12

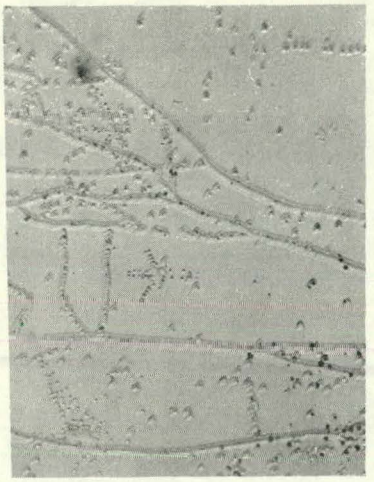

Fig. 13

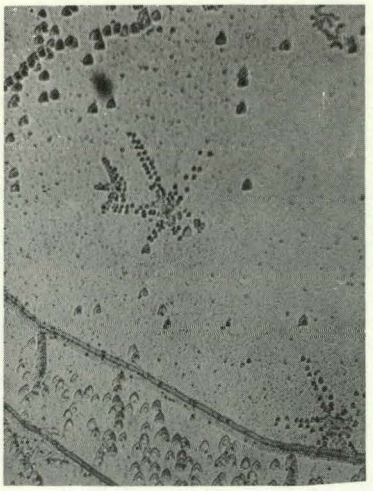

Fig. 14

Fig. 15

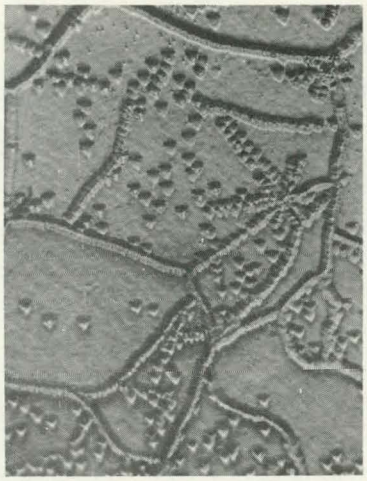

Fig. 16

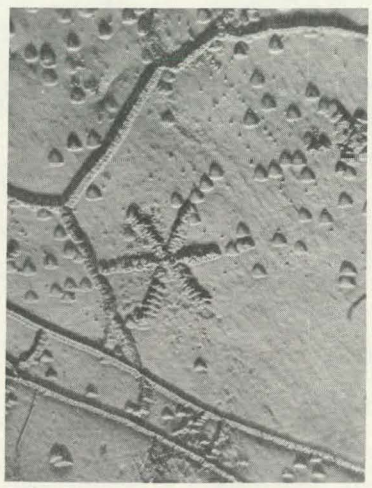

Fig. 17

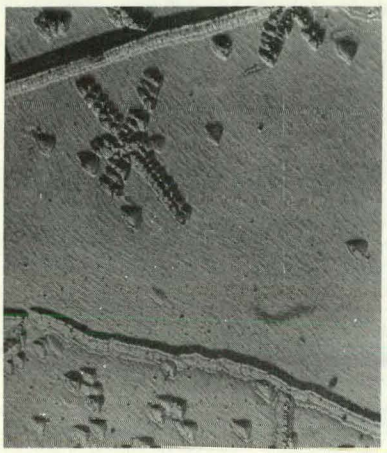

Fig. 18

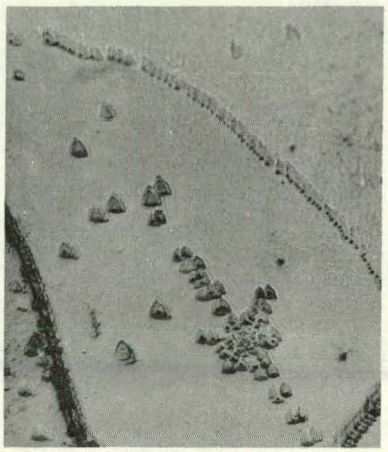

Fig. 19

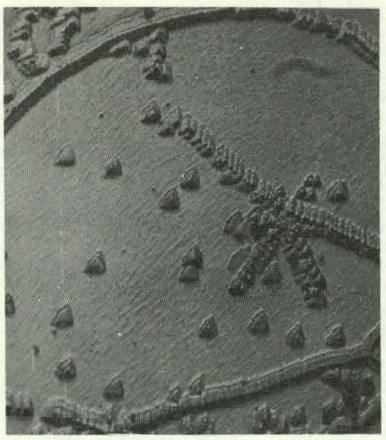

Fig. 20

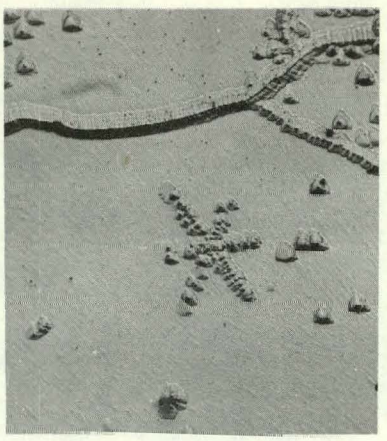

Fig. 21

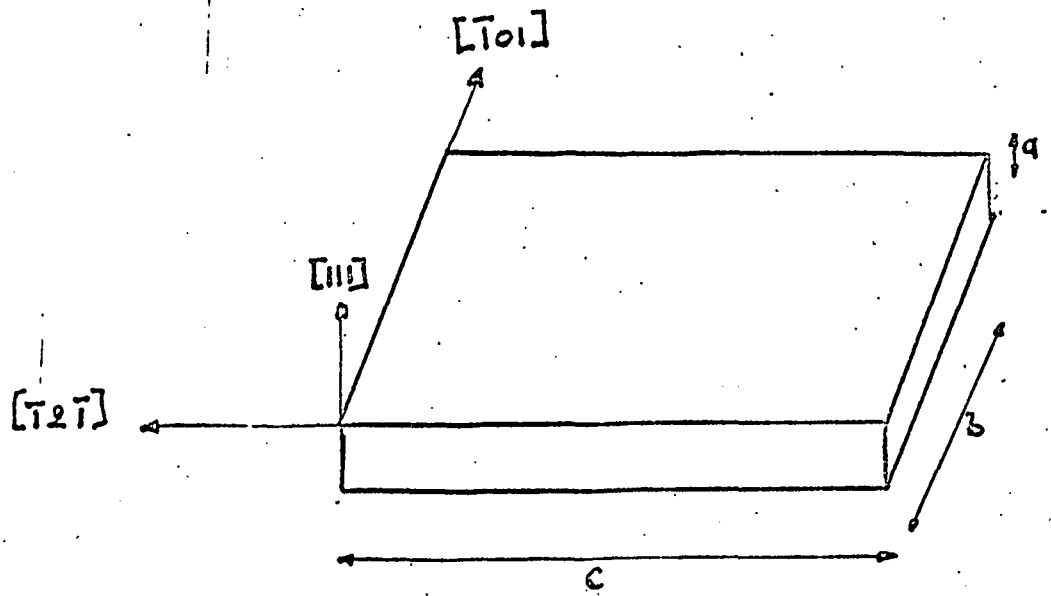

Fig. 22

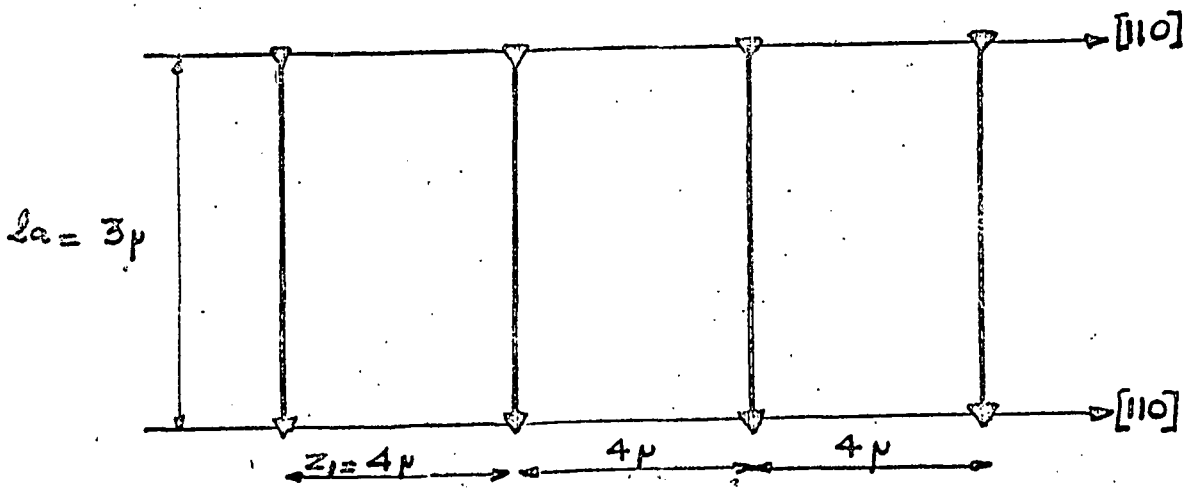

Fig. 23

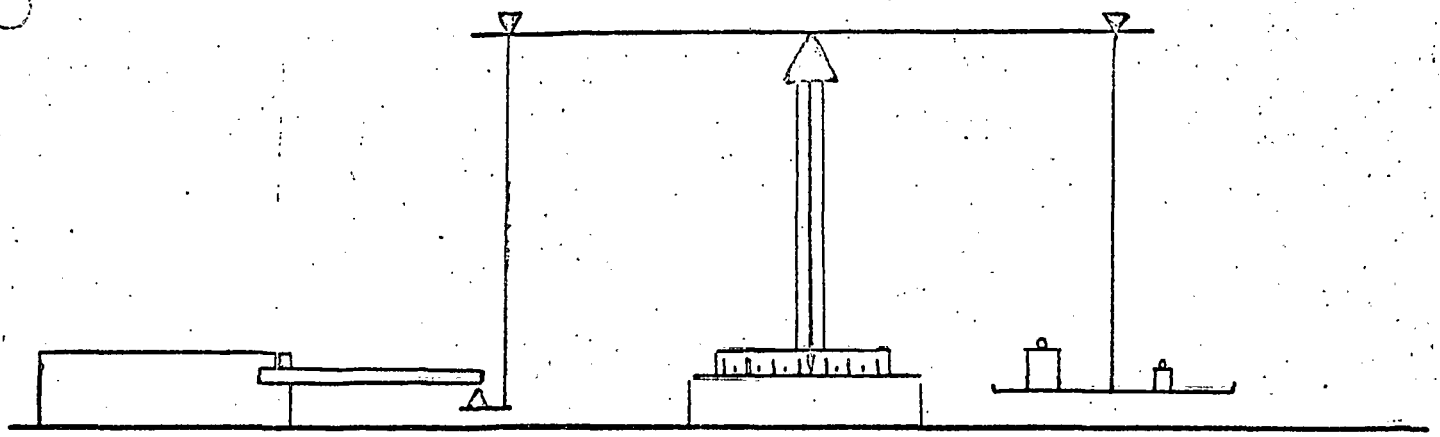

Fig. 24

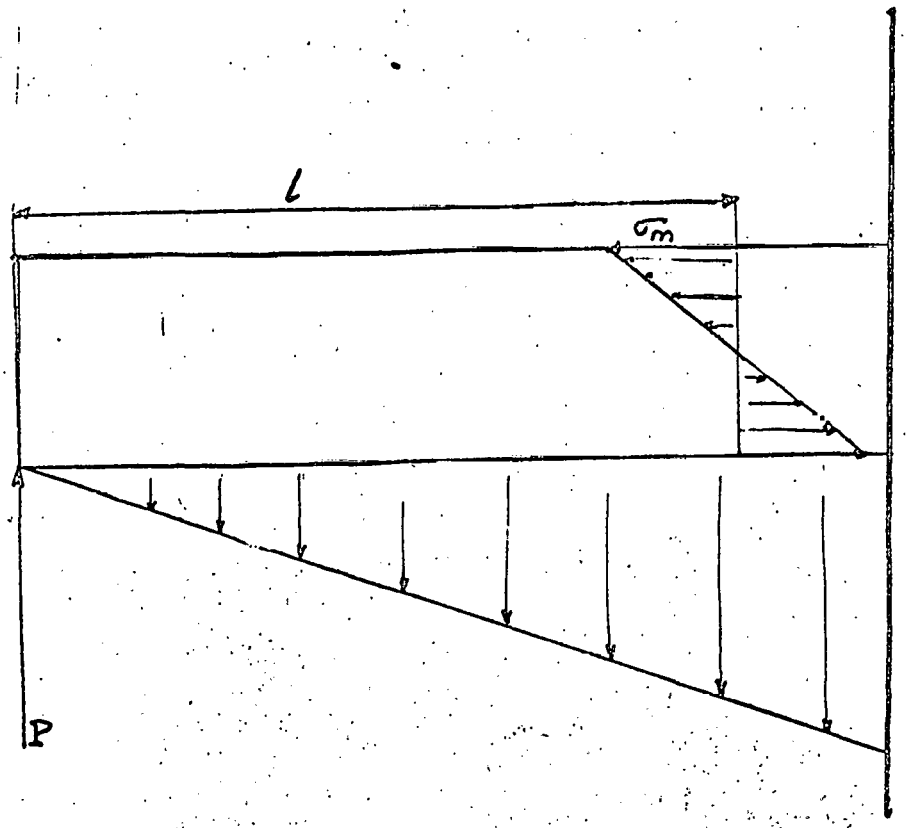

Fig. 25

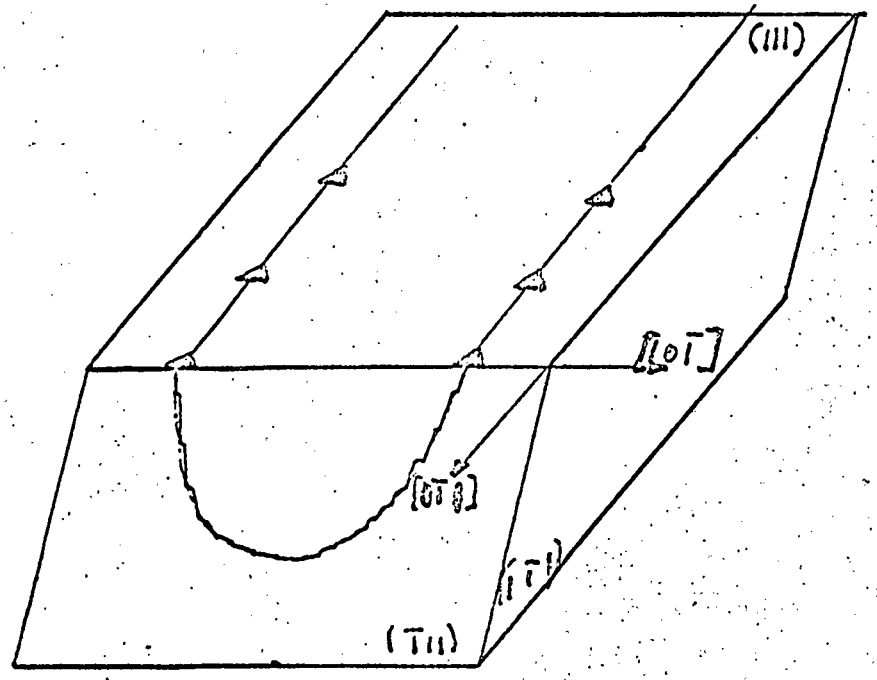

Fig. 26

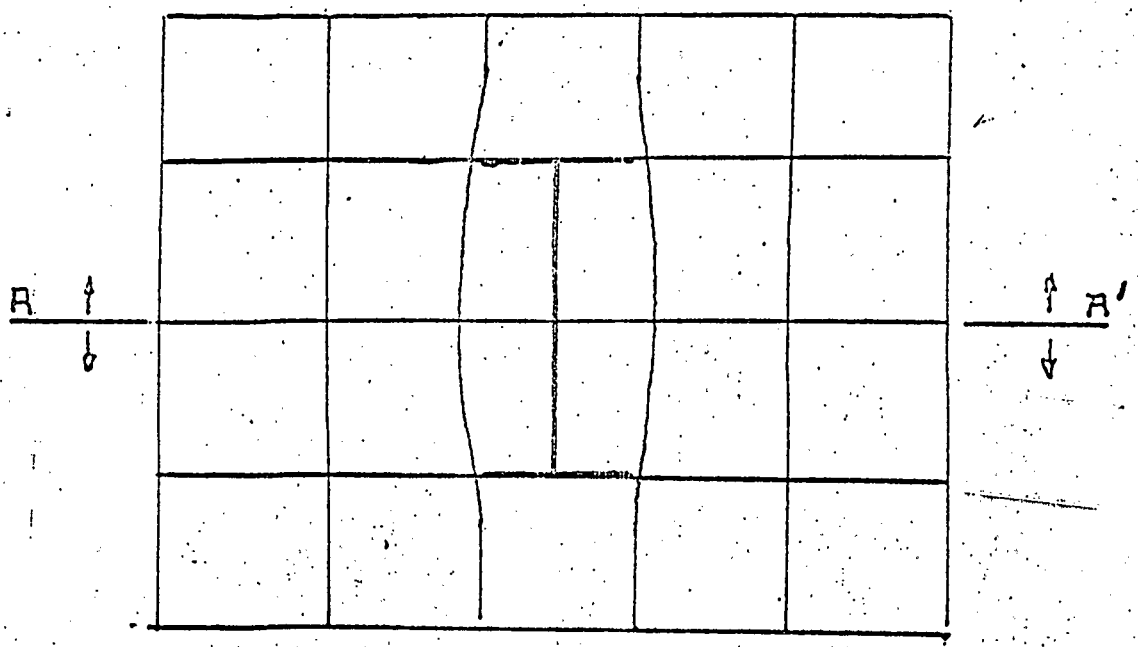

Fig. 27

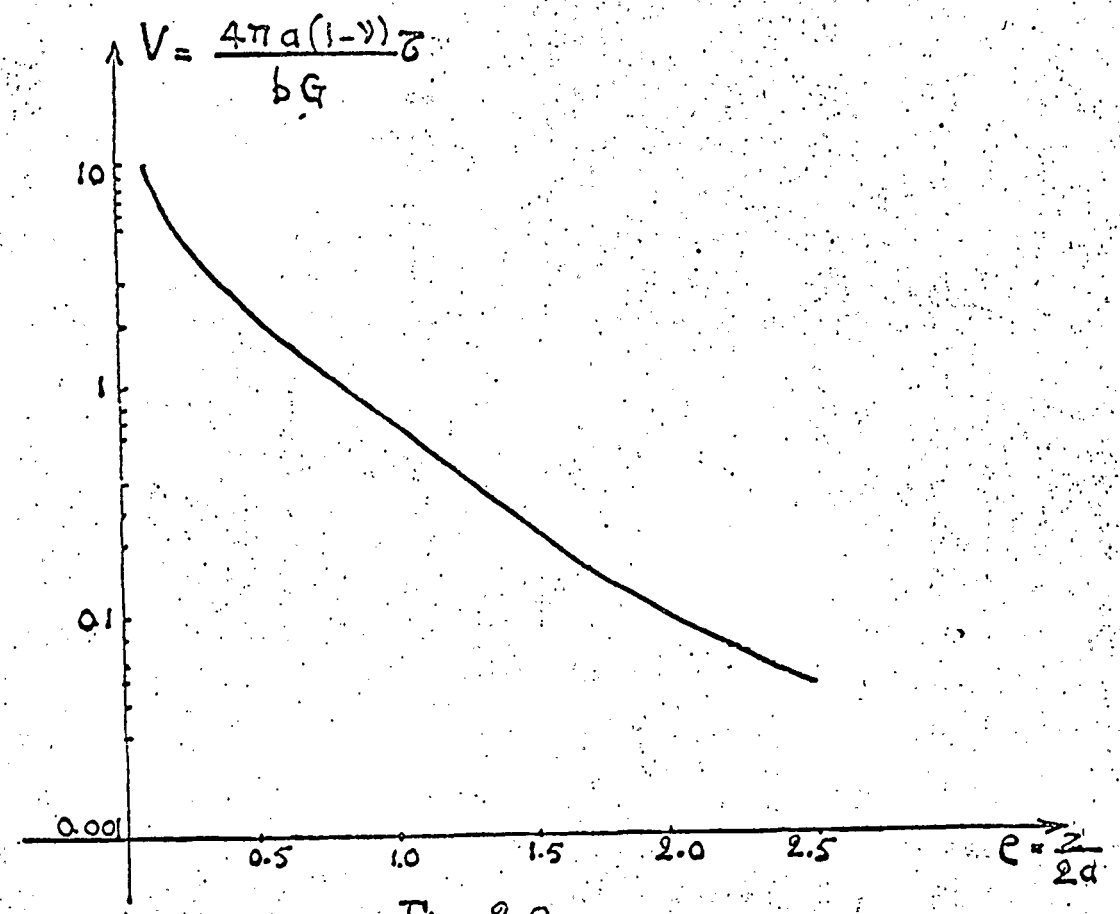
V = 4πa(1-ν)τ / bG
10
1
0.1
0.001
0.5
1.0
1.5
2.0
2.5
e = z/2a

Fig. 28

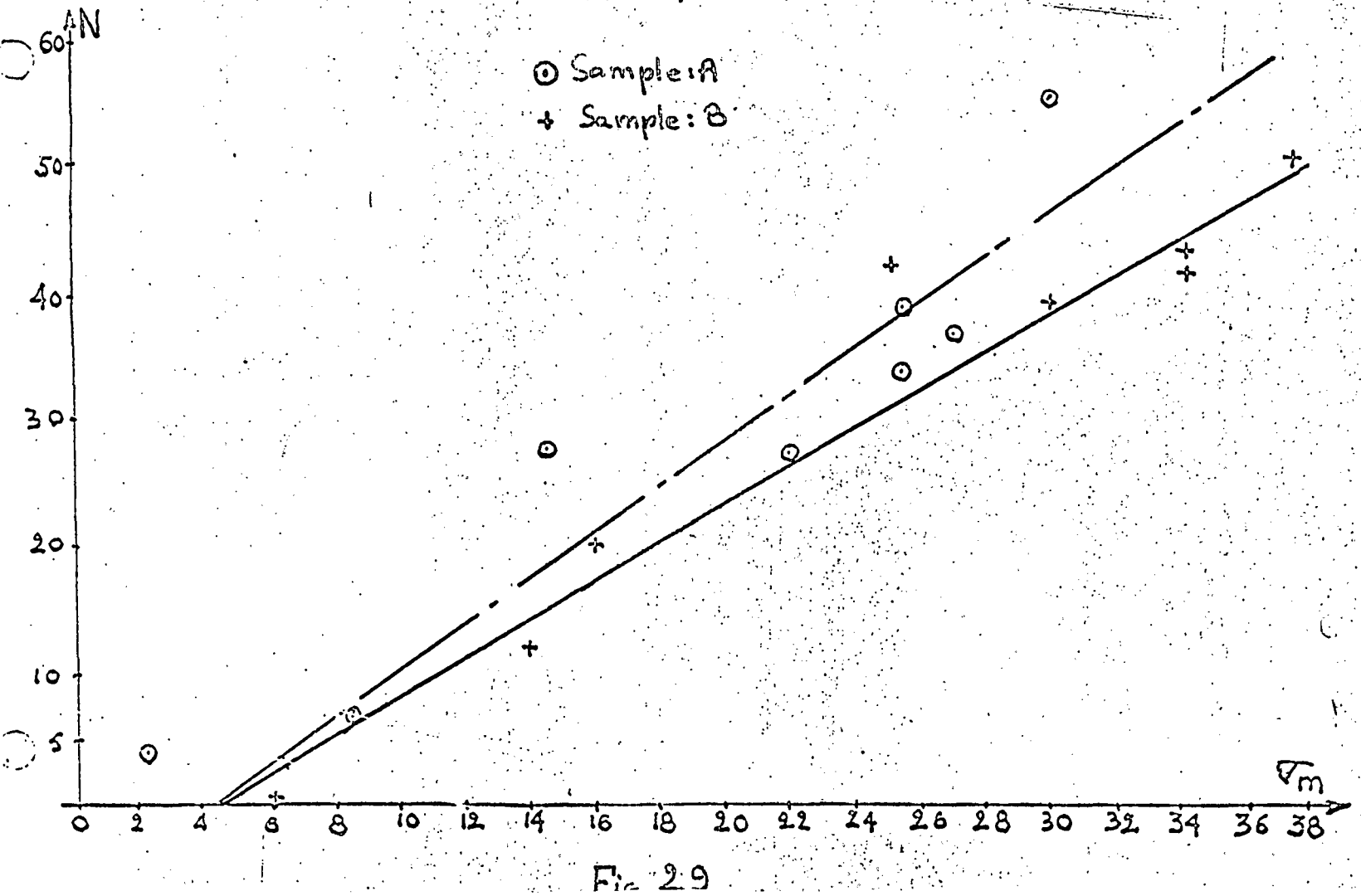
N
60
50
40
30
20
10
5
Sample: A
Sample: B
0
2
4
6
8
10
12
14
16
18
20
22
24
26
28
30
32
34
36
38
Vm

Fig. 29